Classification of Coulombic three-body systems in hyperspherical coordinates

Z. Chen and C. D. Lin
Department of Physics, Kansas State University, Manhattan, Kansas 66506
(Received 24 April 1989; revised manuscript received 9 February 1990)

Hyperspherical coordinates are used to study properties of Coulombic three-body systems of arbitrary masses. Consider a system ABA, which consists of two identical particles A and a third particle B, each with one unit of charge. We examine the evolution of the approximate quantum numbers that are used for classifying bound and resonance states of the system as the mass ratio $\lambda = m_A/m_B$ changes from the atomic limit ($\lambda \to 0$ as in H^-) to the diatomic molecular limit ($\lambda \gg 1$ as in H_2^+). It is shown that for states which exhibit rovibrational behaviors in the atomic limit ($\lambda \to 0$), a single set of approximate quantum numbers can be used to describe three-body systems of any λ's. For states that display independent-particle behavior in the atomic limit, such as singly excited states, it is shown that these states display rovibrational behaviors only in the large-λ limit. The evolution of the spectroscopy of the three-body systems from the shell model of atoms to the rovibrational model of molecules is thus analyzed. Calculations of potential curves in hyperspherical coordinates were carried out for Ps^- and $d^+\mu^- d^+$ that serve as the intermediate steps for the study of the evolution of the approximate quantum numbers from H^- to H_2^+.

I. INTRODUCTION

Since the birth of nonrelativistic quantum mechanics, the "languages," or the approximate quantum numbers for describing atomic systems, are distinctly different from those used for describing molecules. For atoms such as He, the motion of the nucleus can be neglected and the two electrons are described by the independent-electron model (such as the Hartree-Fock approximation). In this model, the motion of each electron is governed by a central potential that is due to the Coulomb attraction of the nucleus and the averaged screening due to the other electron. In other words, the two electrons in the atom are moving more or less independently of each other and there is little "correlation" between them. In the case of molecules, the basic model is the Born-Oppenheimer (BO) approximation, as exemplified by the treatment of the three-body system H_2^+. Within the BO approximation, one takes advantage of the large difference between the masses of protons and electrons, and approximates the wave functions as products consisting of one part describing the rotation and vibration of the two protons as a whole, and another part describing the motion of the electron at each fixed internuclear separation.

The success of the independent-electron approximation for describing atomic systems and the BO approximation for molecular systems proves the basic soundness of each model in its own region of applications. Deviations from each model can often be treated in some form of perturbation theories. However, in the last few decades, it has been shown[1-5] that the independent-electron model fails to describe doubly excited states of atoms. In fact, since the early work of Herrick and collaborators[4,6-8] showing that the energy levels of intrashell doubly excited states of H^- and He exhibit a supermultiplet structure, there have been many theoretical studies[1-27] aiming at the qualitative as well as semiquantitative understanding of these states. Kellman and Herrick[6,7] showed that the intrashell doubly excited states spectra of He could be identified with the rotation and the doubly degenerate bending modes of a symmetric linear triatomic ABA molecule, where the lighter atom A plays the role of an electron and the heavier atom B plays the role of the nucleus. The collective, moleculelike model was substantiated further by Berry and co-workers[5,10-15] by examining the conditional probability distributions of the wave functions in coordinate space and the expectation values of the momentum correlation $\langle \mathbf{p}_1 \cdot \mathbf{p}_2 \rangle$, and by projecting two-electron wave functions into rotor-vibrator functions.

Doubly excited states have also been studied by Lin[1,22,23] and others[9,26-29] in hyperspherical coordinates. Using the adiabatic approximation, it was shown that each potential curve can be labeled with the quantum numbers K and T introduced by Herrick and Sinanoğlu[30] (see also Refs. 20 and 31), together with an additional quantum number A which is similar to the + and − quantum numbers of Cooper, Fano, and Prats.[3] In the hyperspherical approach, both intrashell and intershell states are studied together. it was shown[22,23] that some intershell states do not display rovibrator characters of an ABA molecule. These states, which have been designated with $A=0$, are similar to singly excited states of atoms or to the local modes of a molecule. It was pointed out that these $A=0$ states are not well described by the molecular quantum numbers. Thus the introduction of the A quantum number helps to separate two groups of doubly excited states of atoms: one group which displays rovibrational molecular modes ($A=\pm 1$) and another ($A=0$) which does not.

Another perspective of doubly excited states was taken by Feagin and Briggs.[18,19,24,25] They treated doubly excited states in a manner similar to the BO expansion of

 ©1990 The American Physical Society

H_2^+ by taking the interelectronic distance as the adiabatic parameter. The potential curves thus[24] obtained resemble the hyperspherical potential curves qualitatively and thus the K and T quantum numbers of Herrick and Sinanoğlu[30] can be identified with the molecular orbital (MO) quantum numbers of H_2^+. The relations of the quantum numbers in these different models are summarized in Appendix A.

Despite the equivalence of the quantum numbers used by these models, the accuracy of each model as a first-order description of doubly excited states of atoms remains unclear. Kellman and Herrick[6,7] deduced the linear triatomic molecular model based on the calculated intrashell doubly excited states spectra of He. In particular, the rotor structure for each bending vibrational mode is indeed very striking. However, as studied by Watanabe and Lin,[32] the origin of the rotor structure is not from the kinetic energy as in a triatomic molecule. Instead it was due to the Coulomb repulsion between the two electrons. The truncation of each rotor series in doubly excited states of helium also reflects the effect of the shell structure in atoms. Is the rovibrational energy-level structure of doubly excited states essential for a molecular description? Doubly excited states of Be-like ions have been shown to have no rotor structure,[33] and the discussion of the molecular behavior for alkaline-earth atoms has never referred to the energy levels except for the very limited cases involving valence states.[16] Yet in many respects, such as the electron density distributions,[34] the momentum correlation $\langle \mathbf{p}_1 \cdot \mathbf{p}_2 \rangle$ (Refs. 13 and 14) and the autoionization widths[35] of these atoms are all very similar to those of He-like ions. Similarly, the diatomic molecular picture of Feagin and Briggs fails to point out features of doubly excited states such as the truncation of each rotor series, the rotational contraction along the series, and it fails to include the nonmolecular $A=0$ states. Furthermore, the rotor structure in H_2^+ can be attributed to the kinetic-energy operator, while in intrashell doubly excited states it was mostly due to the Coulomb interactions between the particles.[36]

The relevance of the linear triatomic and diatomic molecular models to the description of doubly excited states of atoms can be explored further from the fundamental interaction level. In the case of helium there are two electrons and one nucleus interacting via Coulomb forces, while in H_2^+ there are two protons and one electron interacting via Coulomb forces. In the linear ABA triatomic molecule where the masses of the atoms are comparable, each pair interacts via a Morse or a harmonic potential. Thus, in the triatomic molecular description the pair interaction potential does not play a significant role in the interpretation of the molecular behavior of atoms. On the other hand, in the diatomic picture, the mass of the two identical particles relative to the mass of the other does not play any role in the interpretation of the molecular behavior of atoms. Thus, from a quantitative viewpoint, one needs to identify what features of the Hamiltonian in each molecular model enter the description of doubly excited states.

In this paper we only attempted to examine how the masses enter into the description of doubly excited states of atoms. To isolate the effect of varying the relative masses, we consider a three-body system of the form ABA, each with one unit of charge. We investigate how the approximate quantum numbers used for describing an atomic system can be reconciled with the quantum numbers for describing a molecule. To do so, it is desirable that a single theoretical method be developed that can be used to calculate accurately the properties of any three-body Coulomb systems. The evolution of the approximate quantum numbers can then be examined as a function of the mass ratio $\lambda = m_A/m_B$, which ranges from the atomic limit ($\lambda \to 0$) to the molecular limit ($\lambda \gg 1$). Meanwhile, this method can be used to calculate properties of specific Coulomb systems such as Ps^- (Refs. 37–39) and muonic molecular ions, including $d^+\mu^- d^+$ and $d^+\mu^- t^+$ (we will use $d\mu d$ and $d\mu t$, respectively, to denote these ions in the rest of this article), which are of interest in the study of muon-catalyzed fusion.[40]

We use mass-weighted hyperspherical coordinates to study Coulombic three-body systems of arbitrary mass. The theoretical method and computational procedure were described in a previous publication.[41] We will outline the methods again in Sec. II and indicate the modifications used in this article. The results are discussed in two sections. In Sec. III we discuss potential curves which converge to the ground state of the two-body system, i.e., of AB. The increase of the number of bound states with the increase of mass ratio λ is interpreted in terms of the increasing attractiveness of the potential curves as λ increases.

To arrive at a complete analysis of the approximate quantum numbers for describing Coulombic three-body systems, one must also examine potential curves which converge to the excited states of the two-body system. This is addressed in Sec. IV. In Sec. IV A we first review briefly the classification scheme of doubly excited states of atoms by Lin and by others. The connection between the K, T, and A quantum numbers for describing the rovibrational motions of the two electrons with the rotation and vibration of molecules is discussed in Sec. IV B. In Sec. IV C we display the potential curves for $^1S^e$, $^1P^o$, $^3P^o$, and $^1D^e$ symmetries for H^-, Ps^-, and $d\mu d$ that converge to the hydrogenic $N=2$ limit. The limitations of the rotor structure and T doubling (or Λ doubling) which are characteristic of molecules are examined, respectively, in Sec. IV D and IV E. A summary and conclusions are given in Sec. V.

II. HYPERSPHERICAL COORDINATE METHOD FOR THREE-BODY PROBLEMS

The hyperspherical coordinates used to describe three-body systems have been discussed previously.[41] In this section we will outline only the essentials to indicate how the calculations are carried out. Starting with the three particles in the center-of-mass frame, three sets of Jacobi coordinates $\{\boldsymbol{\rho}_1^i, \boldsymbol{\rho}_2^i\}$ ($i=\alpha,\beta,\gamma$) can be defined, as shown in Fig. 1. Since we are concerned with three-body systems of the type AAB, we note that the α-set coordinates are similar to those used for molecules where $\boldsymbol{\rho}_1^\alpha$ is the internuclear vector and $\boldsymbol{\rho}_2^\alpha$ is the electronic coordinate. On

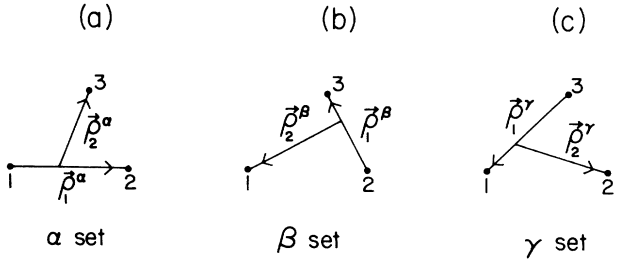

FIG. 1. Jacobi coordinate for three-particle systems. Particles 1 and 2 are identical particles.

the other hand, the β- and γ-set coordinates are closer to those describing atomic systems. Note that if the mass of the nucleus is treated as infinite, then $\boldsymbol{\rho}_1^{\beta}=-\mathbf{r}_1$ and $\boldsymbol{\rho}_2^{\beta}=\mathbf{r}_2$, where $\mathbf{r}_1$ and $\mathbf{r}_2$ are the positions of the two electrons measured from the nucleus. In this limit the β-set and γ-set Jacobi coordinates coincide. The advantage of Jacobi coordinates is that there is no cross term of the type $\nabla_1\cdot\nabla_2$ in the kinetic-energy operator, and that the Schrödinger equation reduces to the two-body dissociation limit with the correct reduced mass.

Starting with each set of Jacobi coordinates we define mass-weighted vectors

$$\xi_1^i=(\mu_1^i/\mu)^{1/2}\boldsymbol{\rho}_1^i , \tag{1a}$$

$$\xi_2^i=(\mu_2^i/\mu)^{1/2}\boldsymbol{\rho}_2^i , \tag{1b}$$

where μ_1^i and μ_2^i are the reduced mass associated with $\boldsymbol{\rho}_1^i$ and $\boldsymbol{\rho}_2^i$, respectively. For each set i, we define a hyperspherical radius R and a hyperangle ϕ (the superscript i has been suppressed),

$$R^2=\xi_1^2+\xi_2^2 , \tag{2a}$$

$$\tan\phi=\xi_2/\xi_1 . \tag{2b}$$

In terms of hyperspherical coordinates, the kinetic-energy operator is rewritten as

$$T=-\frac{1}{2\mu}\left[\frac{\partial}{\partial R^2}+\frac{5}{R}\frac{\partial}{\partial R}-\frac{\Lambda^2(\Omega)}{R^2}\right] , \tag{3}$$

where Ω denotes the five hyperangles, and Λ^2 is the grand angular momentum operator

$$\Lambda^2=-\frac{1}{\sin^2\phi\cos^2\phi}\frac{d}{d\phi}\left[\sin^2\phi\cos^2\phi\frac{d}{d\phi}\right]+\frac{l_1^2(\hat{\xi}_1)}{\cos^2\phi}+\frac{l_2^2(\hat{\xi}_2)}{\sin^2\phi} . \tag{4}$$

The eigenvalues and eigenfunctions of Λ^2 are well known. The advantage of the mass-weighted hyperspherical coordinates is that the hyperradius R is the same for all three sets of Jacobi coordinates, while the eigenfunctions of the $\Lambda^2(\Omega)$ operator have simple transformation properties. Recall that $\Lambda^2(\Omega^{\alpha})=\Lambda^2(\Omega^{\beta})=\Lambda^2(\Omega^{\gamma})$, thus the eigenfunctions for each set of Jacobi coordinates can be obtained from the other through an orthogonal transformation.[42]

We solve the Schrödinger equation in hyperspherical coordinates using the adiabatic approximation with the hyperradius as the adiabatic parameter. Such an approximation has been used in the study of two-electron systems[1,2,9,26–29] and in reactive scatterings.[43] We expand

$$\Psi=\sum_{\nu}F_{\nu}(R)\Phi_{\nu}(R;\Omega) , \tag{5}$$

where the channel function $\Phi_{\nu}(R;\Omega)$ satisfies

$$\left[\frac{\Lambda^2(\Omega)}{R^2}+W(R,\Omega)\right]\Phi_{\nu}(R;\Omega)=U_{\nu}(R)\Phi_{\nu}(R;\Omega) . \tag{6}$$

The potential energy V has been scaled in (6) in the form of $W(R,\Omega)=2\mu V(R,\Omega)$. From the hyperspherical potential curves $U_{\nu}(R)$ the hyperradial equation can be solved to obtain $F_{\nu}(R)$ and its eigenenergy. Our goal in this paper is to present $U_{\nu}(R)$ as a function of the mass ratio λ and to find a set of approximate quantum numbers to designate each channel ν. In principle, a more detailed analysis for the channel index can be obtained by examining the channel wave functions $\Phi_{\nu}(R;\Omega)$. This task is to be undertaken in the future. Furthermore, the potential curves $U_{\nu}(R)$ thus obtained are BO curves since the diagonal coupling terms $\langle\Phi_{\nu}(R;\Omega)|d^2/dR^2|\Phi_{\nu}(R;\Omega)\rangle$ are not included in the curves to be presented below. To obtain accurate energies, the diagonal coupling terms have to be calculated. This has been done for the two-electron system[1,2,9,26–29] and for Ps^- (Ref. 44) when accurate energies are to be calculated.

Each quantum eigenstate of the three-body system is characterized by a set of quantum numbers. Since we do not include spin interactions, the good quantum numbers are the total orbital (L) and spin (S) angular momentum quantum numbers, and the parity π of the system. Following the convention of atoms, the total spin S includes the spins of the two identical particles only. This definition allows us to include the exchange symmetry of the two identical particles conveniently in the wave functions.

Our major computational work is in the solution of Eq. (6). We solve this equation by the eigenfunction expansion method with the basis function given by

$$\Phi(R,\Omega)=\Phi(R;\Omega^{\beta})+(-1)^{l_1^{\beta}+S}\Phi(R;\Omega^{\gamma}) , \tag{7}$$

where we have $\mathbf{L}=\mathbf{l}_1^{\beta}+\mathbf{l}_2^{\beta}$. Equation (7) includes the proper (anti-) symmetrization of the spatial wave function and is applicable to both fermions and bosons systems. The basis functions in the β set and γ set have the same functional form. In the previous work,[41] analytical functions that reduce to hydrogenic wave functions in the limit of large R were used as the basis functions. In this work, we adopt different basis functions. We first assume that l_1 and l_2 are good quantum numbers such that the basis functions can be expressed as

$$\Phi_{l_1l_2q}(R;\Omega^{\beta})=\frac{1}{\sin\phi\cos\phi}g_{l_1l_2q}(R;\phi)\mathcal{Y}_{l_1l_2LM}(\hat{\xi}_1,\hat{\xi}_2) , \tag{8}$$

where the coordinates are in the β set and $\mathcal{Y}_{l_1l_2LM}$ is the

two-particle coupled orbital angular momentum function. The basis functions $g_{l_1 l_2 q}(R;\phi^{\beta})$ at each R are obtained by solving the resulting ordinary differential equation obtained from (6) for each fixed (l_1,l_2). Admixture of different pairs of (l_1,l_2) is carried out by using (7) as basis functions in the rediagonalization of (6). Calculations of matrix elements using this approach were addressed earlier.[41]

The use of β- and γ-set functions allows us to calculate $U_{\nu}(R)$ using a small number of (l_1,l_2) pairs in the expansion since l_1 refers to a bound state of the AB system which has small l_1 for the low-lying states. The l_2 is governed by the triangular relation among l_1,l_2 and L. The number of basis functions within each (l_1,l_2) is also small since prediagonalization has already been carried out in obtaining the basis function. For example, if we are interested in the lowest potential curve for each L, S, and π, we need only up to five basis functions [of $(l_1 l_2 q)$] for the cases considered here. For potential curves which converge to the $N=2$ limit at large R, we need about 15 basis functions. Note that the convergence with respect to the (l_1,l_2) expansion for the low-lying potential curves is relatively fast. For atomic systems it has been shown[26,27] that for potential curves converging to the Nl limit, inclusion of $l_< = \min(l_1,l_2) = N$ is enough to achieve good convergence. For larger λ, a few more (l_1,l_2) pairs are needed. As λ approaches the value ($=1837.0$) for H_2^+, our calculation becomes unreliable. A better approach to such a "molecular" system is to expand the wave function in the body frame. On the other hand, if the wave functions are expressed in the body frame, the structure of the differential equations for different L's are much more complicated. For the purpose of the classification of Coulombic three-body systems here, the present method is much more convenient since the calculations for different L's can be easily carried out without many changes in the code.

III. THREE-BODY BOUND STATES

Before presenting the computational results, we first comment that in all of the calculations presented here, we use $\mu=1$ [see Eq. (3)]. Furthermore, the mass of the lighter particle in the system is always set equal to unity. For example, the mass of muon in $d\mu d$ is equal to unity, while the mass of the deuteron is equal to $m_d/m_{\mu} = 17.7516$. The potential curves thus calculated converge to μ_{AB}/N^2 Ry in the asymptotic limit ($R \to \infty$), where μ_{AB} is the reduced mass of m_A and m_B. In order to facilitate the comparison, we renormalize the potential curves so that each curve converges asymptotically to $-(1/N^2)$ Ry.

A. Potential curves for the $^1S^e$ ground-state channels

In Fig. 2 we show the $^1S^e$ potential curves for a number of three-body systems, including a fictitious system with $\lambda=3$. We note that as the mass ration λ increases, the attractive potential well becomes broader, and we expect that the number of bound states increases slowly. Calculations[45] show that there is only one bound state in

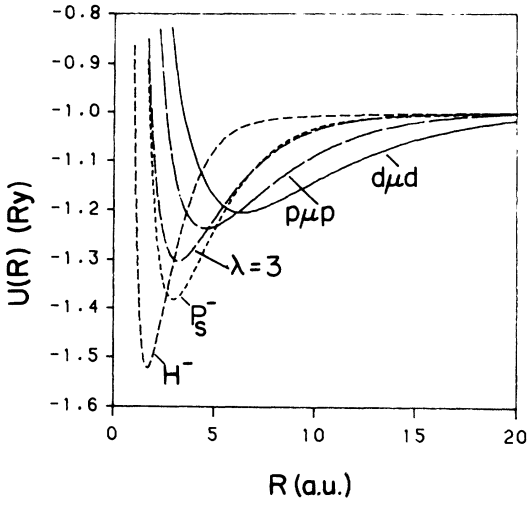

FIG. 2. Hyperspherical potential curves vs the mass ratio λ ($=m_A/m_B$) for the Coulombic three-body systems AAB which consists of two identical particles. The curves shown are for $^1S^e$ symmetry which converge to the $N=1$ hydrogenic dissociation limit. All the curves show an attractive well for all the λ's considered.

the $L=0$ case for H^-, Ps^-, and $p\mu p$, each corresponding to the ground state of the respective system. For $d\mu d$ and $t\mu t$, calculations[45] show that there are two bound states for $^1S^e$. For H_2^+, calculations[46] using the BO potential showed that there are 18 vibrational bound states associated with the $1s\sigma_g$ curve for $L=0$. For L greater than 36, there is no bound vibrational state.[46]

The variation of the potential curves shown in Fig. 2 implies that the binding energy of the ground state increases with λ for $\lambda \geq 1$. Such variations of the ground-state energies with respect to the masses m_A and m_B have been investigated in the literature.[45,47] Most of these studies were based on the variational approaches using Hylleraas-type trial functions. It has been well established that the total binding energy of the AAB system scales almost linearly with the reduced mass μ_{AB} of the two-body ($A+B$) system if the mass ratio $\lambda \leq 1$. The increase in binding for $\lambda > 1$ can be explained in terms of the increasing contributions from the mass polarization term. We discuss this aspect in Appendix B.

B. Potential curves for the lowest $^3P^o$ channels

We next consider the lowest potential curves for the $^3P^o$ symmetry in Fig. 3. For H^-, the potential curve is repulsive in the whole region of R and at large R it can be approximated by $-1.0+2/R^2$. Such a repulsive potential curve does not support any bound states. For Ps^-, we witness that the potential curve begins to show a shallow attractive well. This well is not strong enough to support any bound states, but it is manifested in the much larger $^3P^o$-wave phase shift in e^-+Ps elastic scattering than in e^-+H scattering. In Fig. 4 we compare the $^3P^o$ phase shifts for e^-+H (Ref. 48) and e^-+Ps.[49] We note that the latter phase shift is much

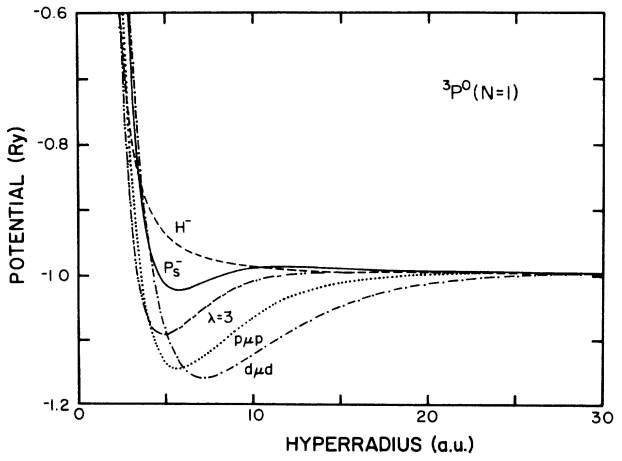

FIG. 3. Same as Fig. 2 except for $^3P^o$. Note that the curves are repulsive for small λ, but are attractive for large λ.

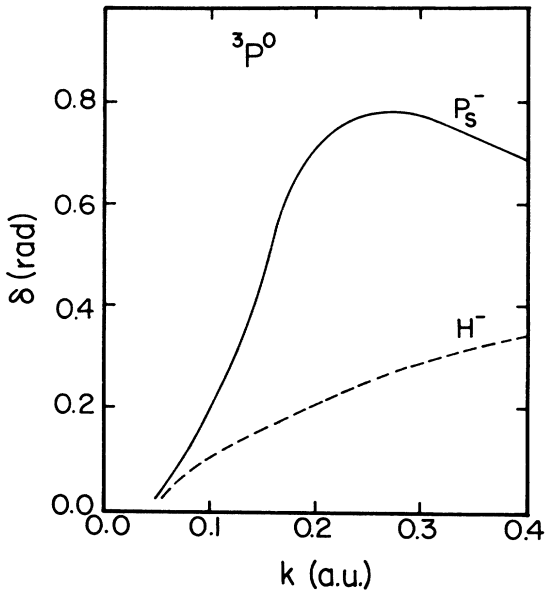

FIG. 4. Comparison of $^3P^o$ elastic scattering phase shifts for e^--H and e^--Ps collisions at low energies. The larger positive phase shift for the latter system is interpreted as due to the stronger effective potential for Ps^- in comparison with H^-. Data from Ref. 48 for H^- and from Ref. 49 for Ps^-.

larger reflecting the shallow attractive potential well shown in Fig. 3.

As the mass ratio λ is increased, the potential curves become even more attractive. For the $p\mu p$ system, there is one bound state[45] (-1.0424 Ry in the reduced units used in the figure), and for $d\mu d$, it is known that there are two bound states[45] (-1.0438 and -1.0074144 Ry in reduced units). In the case of H_2^+, it is estimated[46] that there are 18 bound states within the BO approximation. They are the rotationally excited ($L=1$) vibrational states of the molecules.

C. L dependence of the potential curves

In Fig. 5 we show the potential curves for $^1S^e$, $^3P^o$, $^1D^e$, $^3F^o$, etc. for H^-, Ps^-, and $d\mu d$. These curves are to be compared with the H_2^+ potential curves within the Born-Oppenheimer approximation which are given by $E_s(R)+L(L+1)/2R^2$), where $E_s(R)$ is the electronic energy of the $1s\sigma_g$ orbital and μ is the reduced mass of the two protons. Such a comparison allows us to observe the variation of potential curves with respect to L as the mass ratio λ is varied. We note that in H^-, only the $^1S^e$ curve is attractive. For $e^-e^+e^-$, the $^1S^e$ curve is attractive, while the $^3P^o$ curve, as indicated earlier, shows a slight attractive well at medium R. However, the $^1D^e$ curve and the higher-L curves are all repulsive. For $dd\mu$, the $^1S^e$, $^3P^o$, and $^1D^e$ curves all show attractive wells; the first two are strong enough to support two bound states, but the $L=2$ curve is only attractive enough to support one bound state. The $^3F^o$ curve is slightly attractive and all the higher-l curves are repulsive. These latter curves do not support any bound states.

If the BO description is adequate, then the potential curves for the $L\neq 0$ and $L=0$ states differ only by the rotational kinetic energy. (This result does not hold if the MO curves are calculated beyond the simple BO approximation; see Ref. 24.) This relation is not valid for H^- and Ps^-. For example, in Fig. 6(a) we compare the calculated $^3P^o$ potential curve (in solid line) with the curve (in dashed lines) obtained by adding $2/R^2$ to the $^1S^e$ curve. The two curves would be identical if the BO picture were exact. We note that there is a large discrepan-

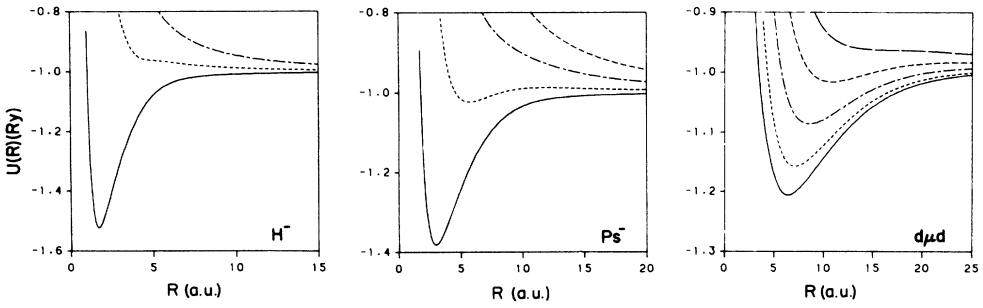

FIG. 5. Potential curves that converge to $N=1$ hydrogenic threshold for H^-, Ps^-, and $d\mu d$ showing the rotational excitations. The lowest curve for each system is for $L=0$, with L increasing by one unit for each successive higher curve.

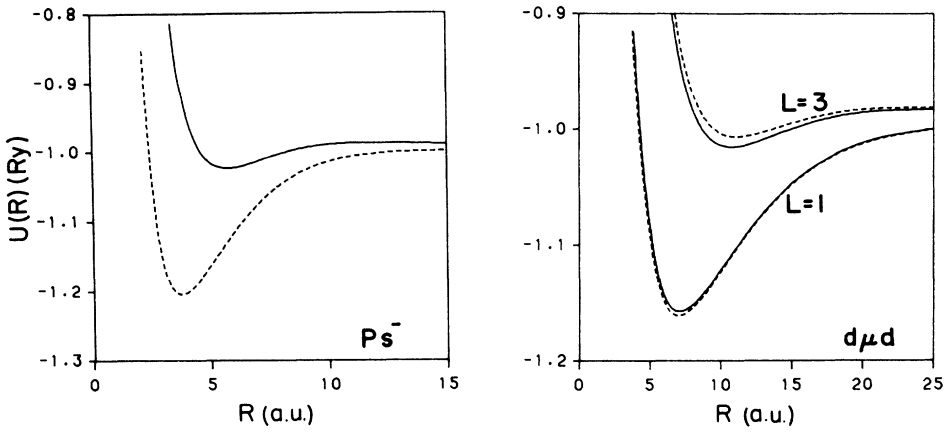

FIG. 6. Validity of the rotor structure for states below the $N=1$ hydrogenic threshold in the dissociation limit. Shown in dashed lines are the potential curves obtained by adding $L(L+1)/R^2$ to the potential of the $^1S^e$ symmetry, and in solid lines are the actually calculated potential curves. If the rotor structure is valid, the two curves for each L should be identical. Potential curves for $L=1$ of Ps^- and $L=1$ and 3 for $d\mu d$ are compared.

cy in the two curves for Ps^-. The situation is markedly different for $d\mu d$ [Fig. 6(b)]. We compare the actually calculated $^3P^o$ and $^3F^o$ curves with the two curves obtained by adding $L(L+1)/R^2$ ($L=1$ and 3, respectively) to the $^1S^e$ curve. We note that in this case the two pairs of curves are much closer to each other, implying that the BO description is quite reasonable.

IV. DOUBLY EXCITED STATES AND CLASSIFICATION OF COULOMBIC THREE-BODY SYSTEMS

As noted in the Introduction, our goal is to examine the approximate quantum numbers for classifying Coulombic three-body systems (of the form ABA) as the relative masses are varied. We need to incorporate the atomic limit ($\lambda \ll 1$), such as H^- and He, as well as the molecular limit ($\lambda \gg 1$), such as H_2^+. The quantum numbers used to describe the states in the two limits are quite different. In the atomic limit, the traditional Hartree-Fock model designates the two-electron states in terms of n, l, N, and l' quantum numbers in addition to the exact L, S, and π quantum numbers. The n, l, N, and l', which are approximate quantum numbers, define the orbitals of the two electrons. In the other extreme ($\lambda \gg 1$), for example, H_2^+, within the BO approximation, the wave function is written as the product of the rotational and vibrational wave functions of the nuclei and the electronic wave functions, which are described in terms of molecular orbitals. The motion of the molecule as a whole is described by a set of quantum numbers, such as the total rotational quantum number L, its projection along the internuclear axis, and the vibrational quantum numbers v. For the electron, its motion is described in terms of molecular orbitals, which are specified in terms of the quantum numbers in the united-atom limit or in the separated-atom limit.

One of the major goals in this study is to establish the evolution of one set of quantum numbers to another as the mass ratio λ is varied. We note that this is different from the quantum numbers relating the united-atom limit to those describing the separated atoms. In the latter case, the internuclear separation is the parameter varied, while in the present case it is the mass ratio λ which is being varied.

Obviously one cannot relate the quantum numbers in the independent-electron model to those used for describing molecules. In the independent-electron model each electron moves independently in a central field provided by the nucleus and the screening of the other electrons, while in molecules such as H^{2+} the two protons are strongly coupled; they rotate together and vibrate around the equilibrium separation with respect to each other. The key to a possible unification for Coulombic three-body problems has occurred only in the last decade with the recognition that atoms in some cases do exhibit behavior similar to the rotations and vibrations of molecules.[6–8] Such rovibrational behavior occurs only when two or more electrons are excited simultaneously. Most of the theoretical studies on this aspect have focused on doubly excited states,[1–25] although preliminary investigations for triply excited states have also been carried out recently.[50,51] We first review the classification of doubly excited states of atoms briefly in Sec. IV A and the diatomic molecular description in Sec. IV B. The adiabatic potential curves for H^-, Ps^-, and $d\mu d$ that converge to the $N=2$ hydrogenic threshold are presented in Sec. IV C to display the variation of the curves with λ. The limitation of the rotor structure and the T doubling of doubly excited states are examined in Sec. IV D and IV E, respectively. We note that specific potential curves in hyperspherical coordinates have been calculated by a different method for a number of cases for Ps^- (Refs. 44 and 52) and for $d\mu d$ (Ref. 53) without the classification scheme in mind.

A. Classification of doubly excited states of atoms

There is a relatively large volume of literature for describing the rovibrational motion of doubly excited

states of atoms today. However, it is also recognized[1,22,23] that singly excited states and some doubly excited states of atoms do not display the rovibrational motion characteristic of triatomic molecules. To incorporate all possible states of a two-electron atom, we follow Lin[1,22,23] and designate each state by ${}_n(K,T)^A_N {}^{2S+1}L^\pi$. The L, S, and π are exact quantum numbers for the Coulombic three-body systems considered here. The other quantum numbers K, T, and A, as well as n and N, are approximate quantum numbers. From the independent-electron model viewpoint, $(K,T)^A$ replaces l and l'; the superscript A is used to imply that A is not independent of K and T. In this designation, n and N are to retain the usual meaning in the independent-electron model, being the principal quantum numbers of the outer and the inner electrons, respectively.

In terms of this classification scheme, doubly excited states are divided into two classes, one with $A=\pm 1$ and the other with $A=0$. States that are designated by $A=\pm 1$ exhibit properties similar to the rotation and vibration of molecules. The quantum number K, which describes the angular correlation of the two electrons with respect to the nucleus, is similar to the bending vibrational quantum number v of a triatomic molecule. In fact, $v=N-K-1$.[7,32] The quantum number T is the projection of L along the interelectronic axis, which is similar to the projection of the rotational angular momentum along the body frame of a molecule. From such a molecular viewpoint, n describes the stretching vibrational excitations, N describes the dissociation limit and corresponds to the principal quantum number in the separated-atom limit. The other class of states, designated by $A=0$, are similar to singly excited states where the two electrons are more or less independent. They do not behave like molecules and the quantum numbers K and T serve only as indices for labeling the states.

According to this classification scheme, the spectroscopy of doubly excited states exhibits interesting features. For states with $A=0$, it has been shown[1,22] that the energy levels display regular spectral features similar to those seen for singly excited states. For each n, N, K, T, L, and π, the energy level of the triplet state is always lower than the singlet if $\pi=(-1)^L$ and opposite if $\pi=(-1)^{L+1}$. For doubly excited states with $A=\pm 1$, the spectral regularity is characteristic of the rotor-vibrator spectra of molecules.[1,6-8] Within a given n, N, K, and T (similar to a given stretching and bending vibrational mode), the energy levels of successive L's form a rotor series. In addition to the rotor structure, these doubly excited states also display T doubling, which is similar to the Λ doubling in molecules. The latter occurs for each pair of near-degenerate states which have identical n, N, K, T ($\neq 0$), and L (but opposite S and opposite π). Extensive discussions of the rovibrational behavior of doubly excited states of atoms have addressed in the literature.[1,6-8,32] More careful examinations of the properties of doubly excited states of atoms reveals a number of differences from the typical rovibrational behavior of molecules reflecting the shell structure of atoms. Such differences will be addressed further in Secs. IV D and IV E below.

B. Classification of doubly excited states of atoms using diatomic MO quantum numbers

Doubly excited states of atoms have been classified in terms of diatomic molecular quantum numbers by Feagin and Briggs.[18,19,24,25] By treating the interelectronic axis in atoms similar to the internuclear axis in H_2^+ and assuming that the projection of L along the interelectronic axis is a good quantum number as in the BO approximation, they showed that doubly excited states of atoms can be classified using the same set of quantum numbers that describes H_2^+. In this "diatomic" molecular picture (which is different from the linear triatomic molecular picture[6-8]), both K and T can be related to the molecular quantum numbers of H_2^+. Recall that within the BO approximation, the electronic wave function is separable in spherodial coordinates λ, μ, and ϕ. The number of nodes N_λ, N_μ, and m for each of the coordinates is fixed as the internuclear distance is changed. Thus one can relate N_λ, N_μ, and m to the united-atom quantum numbers n, l, and m or to the separated-atom quantum numbers n_1, n_2, and m (which are the hydrogenic quantum numbers in parabolic coordinates). The K, T, and A are related to these by $T=|m|$, $K=n_2-n_1$, and $A=(-1)^N\mu$.[24] In Appendix A the quantum numbers and their relations used in the different models of atoms are summarized.

Feagin and Briggs also labeled each MO with a gerade ($t=+1$) or an ungerade ($t=-1$) symmetry quantum number t. Since $t=\pi(-1)^S$ where both π and S are good quantum numbers, t is also a *good* quantum number independent of the BO approximation. This is not to be confused with the A quantum number defined in the $(K,T)^A$ classification scheme where A is referring to the symmetry of the wave function in the body frame under the exchange of the two identical particles. A is an approximate quantum number while t is an exact quantum number replacing π and S.

Within such a BO approximation the potential curves for all three-body systems considered here can be scaled from the BO curves of H_2^+. The resulting BO potential curves[24] show some resemblance to the potential curves calculated in hyperspherical coordinates, although there are important quantitative and qualitative differences. In the treatment of Feagin and Briggs, the projection of L along the interelectronic axis (quantum number T) is treated as a good quantum number. In the hyperspherical approach, no such assumption was made. The analysis of Watanabe and Lin[32] of the wave functions calculated in hyperspherical coordinates showed that T is only an approximate quantum number. This accounts for most of the qualititive differences between the BO approach and the hyperspherical approach of doubly excited states of atoms. The other difference is that the BO approach does not give correct asymptotic potential curves in the separated atom limit, although this can be improved by solving the potential curves including the second-order diagonal coupling term nonperturbatively.[19,24]

C. Potential curves that converge to the hydrogenic $N=2$ threshold for H^-, Ps^-, and $d\mu d$

In Figs. 7–10 we show the $^1S^e$, $^3P^o$, $^1D^e$, and $^1P^o$ potential curves of H^-, Ps^-, and $dd\mu$ that converge to the hydrogenic $N=2$ limit. Similar to the potentials shown earlier, all the curves in Figs. 7–10 are normalized so that they all approach -0.25 Ry in the asymptotic limit. The potential curves for H^- are labeled according to the $(K,T)^A$ designations, while the $dd\mu$ curves are labeled with the H_2^+ molecular orbitals using the united-atom molecular quantum numbers n, l, and $|m|$. For Ps^-, we choose to label the curves as in H^- since in many respects Ps^- is similar to H^-.

In Fig. 7 for $^1S^e$ there are two curves converging to the hydrogenic $N=2$ limit; one has an attractive potential well, the other is completely repulsive. The attractive $(1,0)^+$ curve corresponds to the bonding $3d\sigma_g$ MO, while the repulsive $(-1,0)^+$ corresponds to the $2s\sigma_g$ orbital. Since $L=0$, the projection of L onto the axis of the two identical particles is also a good quantum number, i.e., $T=0$. As the mass ratio λ increases, the lower potential curve becomes shallower but much broader, extending to larger values of R. The increase in the range of R of course is related to the fact that we use a mass-weighted hyperradius. The repulsive curve remains repulsive for all the λ considered. We note that this curve is also repulsive for H_2^+ in the BO approximation.

In Fig. 8 we consider the three $^3P^o$ curves that converge to the hydrogenic $N=2$ limit. For H^- and Ps^-, the three curves are labeled $(1,0)^+$, $(0,1)^-$, and $(-1,0)^0$, and for $d\mu d$ they are labeled $3d\sigma_g$, $3d\pi_g$, and $2s\sigma_g$, respectively. Since $L=1$, the projection of L onto the axis of the two identical particles can have $T=0$ and 1. As in atoms, the use of $A=0$ is to indicate that T is not a good quantum number, meaning admixture from the $T=0$ and 1 components is quite large. The $(1,0)^+$ curve indicates that $T=0$ is the dominant component, and $A=+1$ means that the wave function in the body frame is symmetric with respect to the interchange of the two identical particles. For the $(0,1)^-$ curve, $T=1$ is the dominant component and the wave function in the body frame is antisymmetric with respect to the interchange of the two identical particles ($A=-1$). The symmetry properties of the wave function with respect to the interchange of the two identical particles are not explicitly given in the MO designation. (In the BO approximation, the electronic potential curves for H_2^+, HD^+, and D_2^+ are all identical.) Note that the two $(1,0)^+$ and $(-1,0)^0$ curves (or $3d\sigma_g$ and $2s\sigma_g$) have the same K and T labels as in $^1S^e$. In terms of the molecular picture, the $(1,0)^+$ $^3P^o$ curve is the rotational excited ($L=1$) curve of $(1,0)^+$ $^1S^e$, and both have the same $3d\sigma_g$ designation. For $d\mu d$, the potential curves are designated using MO quantum numbers and the two curves $2s\sigma_g$ and $3d\pi_g$ are allowed to cross.

The presentation of diabatic curves in Fig. 8 for $d\mu d$ instead of the adiabatic curves actually calculated deserves some discussions. This diabatic crossing of curves is based on the expectation that the narrowly avoided crossing will effectively become a real crossing in the solution of the full problem. Diabatic crossing between the two curves also occurs if the projection of L along the d-d axis is treated as a good quantum number such that σ and π curves can actually cross, as in the BO approximation where the distance between two deuterons is the adiabatic parameter. For Ps^-, we do not allow the two corresponding curves $(0,1)^-$ and $(-1,0)^0$ to cross since T, the projection of L along the interelectronic axis, is only an approximate quantum number for the upper curve ($A=0$) and thus the noncrossing rule applies. If T were assumed to be a good quantum number, as in Feagin and Briggs, the two curves would also cross as in $d\mu d$.

In Fig. 9 we show the three $(1,0)^+$, $(0,1)^0$, and $(-1,0)^0$ curves (or the $3d\sigma$, $3d\pi$, and $2s\sigma$ curves for $d\mu d$) for $^1D^e$, which are similar to those for $^3P^o$. The designation of $(0,1)^0$ indicates that this curve does not have the dominant $T=1$ component any more. This is also reflected by the larger separation between the $(0,1)^0$ and $(-1,0)^0$ curves in comparison with the two corresponding curves in $^3P^o$. On the other hand, the three curves for $d\mu d$ are very similar to those for $^3P^o$ except that each curve is excited with one more unit of rotational angular momentum.

In Fig. 10 we show the three $^1P^o$ curves that converge to the hydrogenic $N=2$ threshold. The curves are labeled $(0,1)^+$, $(1,0)^-$, and $(-1,0)^0$ for H^- and Ps^-, and $2p\pi_u$, $4f\sigma_u$, and $3p\sigma_u$ for $d\mu d$. The designation of $(0,1)^+$ and $(1,0)^-$ indicates that T and A are approximate good quantum numbers for H^- and Ps^- and the two curves are allowed to cross. Similarly for $d\mu d$ the $2p\pi_u$ and $4f\sigma_u$ curves are allowed to cross because they belong to $T=1$ and 0, respectively. For $d\mu d$, the $3p\sigma_u$ labeling implies that $T=0$ is a good quantum number. On the other hand, the $(-1,0)^0$ labeling for H^- and Ps^- implies that $T=0$ has a strong mixture with the $T=1$ component.

From the above examples we conclude that the nature of the approximate quantum numbers is used to decide adiabatic or diabatic crossings in presenting hyperspherical potential curves, although adiabatic curves are actually calculated. In the MO picture, since T is assumed to be a good quantum number, all the adiabatic curves which have different T can cross. (For H_2^+, crossing also occurs for some curves with identical T within the BO approximation.[54]) This explains the origin of the differences between the MO curves of Feagin and Briggs[24] and the hyperspherical curves for atoms; see, for example, Figs. 3 and 4 of Ref. 24.

D. Rotor structure

According to the $(K,T)^A$ classification scheme for H^-, the lowest states for each of the $(1,0)_2^+$ $^1S^e$, $^3P^o$, and $^1D^e$ curves form a rotor series, while for molecules such as H_2^+ the number of rotor states for each electronic curve is quite large. For atoms (H^- and He) these are the only three rotor states for the $N=2$ intrashell doubly excited states, corresponding to $2s^2\,^1S^e$, $2s2p\,^3P^o$, and $2p^2\,^1D^e$ in the independent-particle designation. Thus for *atoms the number of states in a rotor series still reflects the shell structure,* while for molecules this is not the case. How

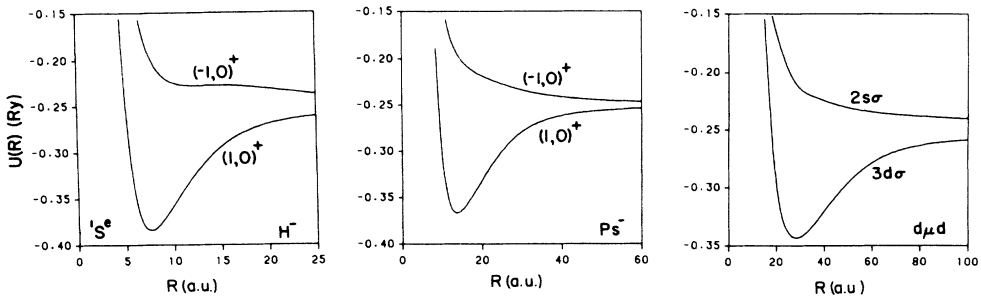

FIG. 7. Potential curves for $^1S^e$ symmetry that converge to the $N=2$ hydrogenic limit. For H^- and Ps^-, each curve is labeled with the K, T, and A quantum numbers used previously for atoms. For $d\mu d$, the MO quantum numbers are used to label the curves.

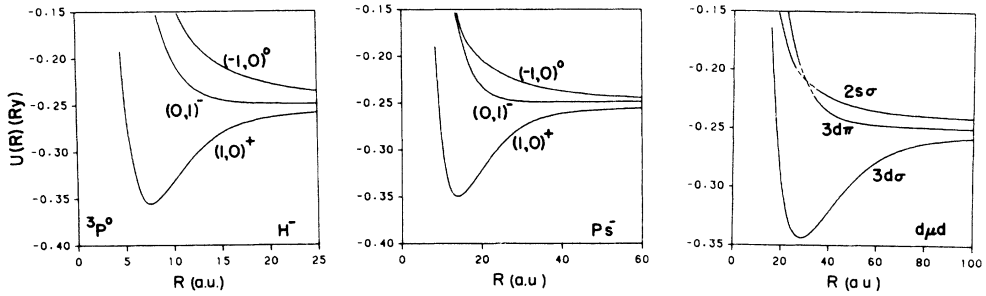

FIG. 8. Same as Fig. 7 except for $^3P^o$. For the discussion of crossing or noncrossing between the curves, see text.

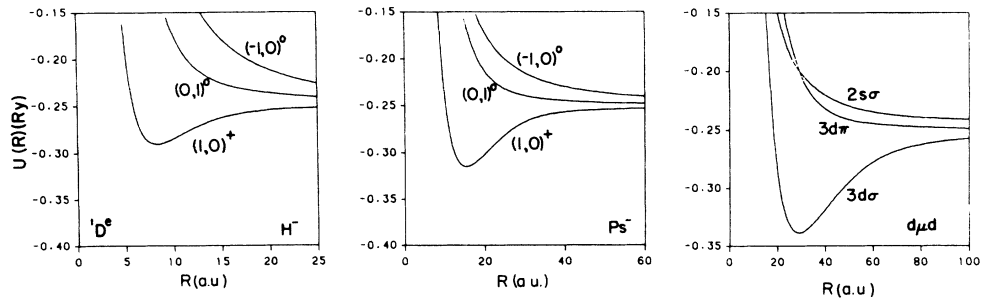

FIG. 9. Same as Fig. 7 except for $^1D^e$.

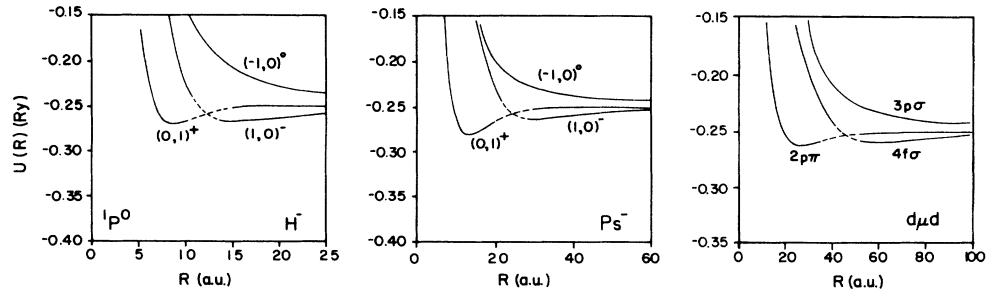

FIG. 10. Same as Fig. 7 except for $^1P^o$.

does the rotor structure vary as the value of λ changes?

Within the BO approximation, the potential curves associated with the higher members of a rotor series can be obtained from the $L=0$ curve by an additional rotational kinetic-energy term $L(L+1)/R^2$. In Fig. 11(a) we compare the $(1,0)^+\,{}^3P^o$ and $(1,0)^0\,{}^3F^o$ curves of Ps^- actually calculated (in solid lines) with those obtained by adding $L(L+1)/R^2$ $(L=1,3)$ to the calculated $(1,0)^+\,{}^1S^e$ curve (in dashed lines). We note that the two ${}^3P^o$ curves agree quite well, indicating that the rotor structure model is quite reasonable. [We remark again that this is not the case for the lowest ${}^3P^o$ curve; see Fig. 6(a).] However, for ${}^3F^o$, the two curves differ significantly; the actually calculated curve lies much higher. We have checked that for ${}^1D^e$ the corresponding two curves are similar to those for ${}^3P^o$, while for $L\geq 4$ they are similar to ${}^3F^o$. This is consistent with the $(K,T)^A$ classification scheme that ${}^3F^o$ and higher L curves are not members of the rotor series since for $N=2$ the series terminates at ${}^1D^e$. This indicates that the rotor structure also terminates at ${}^1D^e$ for Ps^-. In Fig. 11(b) we show a similar comparison for $d\mu d$. It is clear that the rotor structure extends beyond $L=3$ and that the termination of the rotor structure due to the shell model does not apply to $d\mu d$ any longer. The $d\mu d$ system resembles H_2^+ and the rotor structure extends to higher L's.

E. T doubling

Another feature of the $(K,T)^A$ classification scheme is T doubling. This occurs for rovibrational states (those with $A=\pm 1$) which have identical K, T, A, and L (but different S and π). For example, in the case of H^-, the ${}_2(0,1)_2^+\,{}^1P^o$ and the ${}_2(0,1)_2^+\,{}^3P^e$ states (or the $2s2p\,{}^1P^o$ and $2p^2\,{}^3P^e$ states in the independent-particle notation) are nearly degenerate. If the wave functions of these two states are analyzed in the body frame of the atom, to first order the two wave functions are identical and the energies of the two states are degenerate. The T doubling, corresponding to the Λ doubling in diatomic molecules, is the result of the fact that T is not an exact quantum number. In the present example, $T=1$ is an exact quantum number for ${}^3P^e$, but for ${}^1P^o$, $T=1$ is only an approximate quantum number which has a small admixture of the $T=0$ component. It turns out that the small $T=0$ admixture has a profound effect on the energy spectrum of H^-. Although the two potential curves are nearly degenerate, the small T doubling results in that the ${}^1P^o$ state is a shape resonance above the $n=2$ threshold while the ${}^3P^e$ state is a bound state with energy slightly below the $n=2$ threshold.[55] Such results as obtained using hyperspherical coordinates are in agreement with experimental data and with other calculations.

An interesting question is how the T doubling varies with the mass ratio λ. We have also calculated the $(0,1)_2^+$ potential curves for ${}^1P^o$ and ${}^3P^e$ of Ps^-. It turns out that the two potential curves are practically identical, and that they are not strong enough to support any bound states. Therefore the so-called $2p^2\,{}^3P^e$ state, which is a bound state in H^-, is no longer bound for Ps^-, but rather a shape resonance. Since the width of the shape resonance is determined by the potential barrier penetration, the energies and the widths of these two states are expected to be very close. This result has been addressed by Botero and Greene.[44] We further mention that the existence of the $2p^2\,{}^3P^e$ bound state as a function of the mass ratio λ has been studied using variational calculations.[47] It was concluded that this state is not bound for $0.3<\lambda<17.0$. We emphasize that within this range of λ, this state should be a shape resonance.

V. SUMMARY

In this paper we examined the classification of Coulombic three-body systems in which two of the particles are identical, each with one unit of charges. By ex-

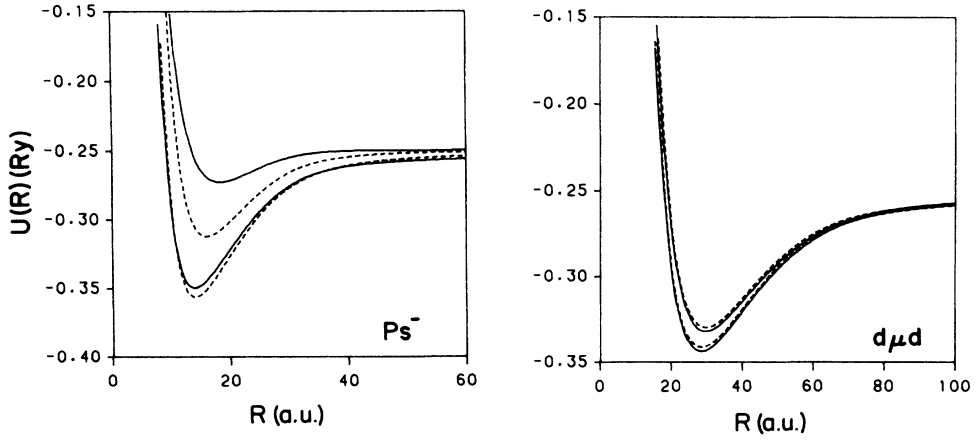

FIG. 11. Validity of the rotor structure for states converging to the $N=2$ hydrogenic threshold. The dashed lines are obtained by adding $L(L+1)/R^2$ to the ${}^1S^e$ potential curve, while the solid lines are from the actual calculations. The general agreement between each pair of curves which have identical L implies the validity of the rotor structure. The two pairs of curves considered are $L=1$ and 3. See text for the discussion of the termination of the rotor series. The curves considered are labeled as $(1,0)^+$ or $3d\sigma$.

panding the wave functions in mass-weighted hyperspherical coordinates we examined the evolution of the approximate quantum numbers from those used for describing atomic three-body systems to those for describing molecular three-body systems. Specific calculations were carried out for hyperspherical potential curves for H^-, Ps^-, and $d\mu d$ for states which converge to the $N=1$ and 2 hydrogenic limits.

It is shown, as in Feagin and Briggs, that for the purpose of labeling states of a three-body Coulombic system, there is a one-to-one correspondence between the $(K,T)^A$ scheme used for describing the atomic systems ($\lambda \ll 1$), the rovibrational quantum numbers (v,T) for a linear triatomic molecule ($\lambda \cong 1$), and the molecular orbital quantum numbers used in the H_2^+ limit ($\lambda \gg 1$). This one-to-one relation is based on the assumption that the projection of the total orbital angular momentum along the line joining the two identical particles is a good quantum number. This assumption is valid in the diatomic molecular limit such as in H_2^+ within the Born-Oppenheimer approximation, but deviations increase in general as λ decreases. For a certain class of states, however, these molecular behaviors remain quite prominent even as $\lambda \to 0$ (i.e., in the atomic limit). These states are the doubly excited states labeled with $A=\pm 1$ in the $(K,T)^A$ classification scheme. For these states, one can use the other two equivalent descriptions and the spectra of these states do exhibit typical molecular characters such as rotor structure and T doubling. On the other hand, the $(K,T)^A$ classification scheme does emphasize that the $A=0$ states do not display molecular behaviors in the $\lambda \to 0$ limit. For these latter states, the K and T serve as labels only since neither are approximate good quantum numbers. However, they serve as the correct molecular quantum numbers in the molecular limit, i.e., when $\lambda \gg 1$. By examining the rotor structure of the potential curves for Ps^- and $d\mu d$ we show the gradual evolution of the $A=0$ states to the molecular limit. We note that the present hyperspherical approach does provide a method for calculating all the states of a three-body Coulombic system.

There remains at least one more relevant question in the general characterizations of three-body systems. One notes that the interpretation of doubly excited states of atoms in terms of a linear triatomic molecule implies that the rovibrational behavior of a three-body system is not very sensitive to the interaction potentials in the system. Thus it is desirable to study the rovibrational behaviors of a three-body of arbitrary masses with different interaction potentials. Since the present hyperspherical approach is not limited to Coulombic potentials, such a study is readily feasible. We comment that a similar study for a model system of two particles on a spherical surface has been carried out by Ezra and Berry.[56]

ACKNOWLEDGMENTS

This work is supported in part by the U.S. Department of Energy, Office of Basic Energy Sciences, Division of Chemical Sciences.

APPENDIX A: RELATION BETWEEN THE DIFFERENT CLASSIFICATION SCHEMES OF DOUBLY EXCITED STATES OF ATOMS

There are a number of classification schemes where approximate quantum numbers are used to designate doubly excited states of atoms. In the classification scheme of Lin,[1] which adopted the K and T quantum numbers of Herrick and Sinanoğlu,[30] and the + and − quantum numbers of Cooper, Fano, and Prats,[3] each doubly excited state is designated by ${}_n(K,T)^A_N$, in addition to the usual L, S, and π quantum numbers. Subsequent works by Herrick and co-workers[6-8] and by Berry and co-workers[5,11-15] demonstrated that the energy levels of intrashell ($n=N$) doubly excited states of atoms resemble the rovibrator pattern of a linear triatomic molecule. The relation between the K and T quantum numbers of atoms and the vibrational angular momentum l_v and bending vibrational quantum number v_2 of a linear triatomic molecule is[7]

$$N-K-1 \leftrightarrow v_2 \ , \qquad T \leftrightarrow l_v \tag{A1}$$

(l_v is used here to avoid confusion with the l used for the orbital angular momentum of the electron). There are a number of differences in the spectra of doubly excited states of atoms and the rovibrational spectra of a linear triatomic molecules, as discussed by Kellman and Herrick[7] and by Watanabe and Lin.[32] The latter paper also studied the "goodness" of the quantum numbers K and T for doubly excited states by examining the wave functions calculated in hyperspherical coordinates.

In the hyperspherical approach for two-electron atoms, a Born-Oppenheimer-type approximation was used, with the hyperradius $R=(r_1^2+r_2^2)^{1/2}$ as the adiabatic parameter, and each potential curve (or channel) labeled by the quantum numbers K, T, and A. The two-electron atoms have also been treated by Feagin and Briggs[18,24] in a manner similar to the Born-Oppenheimer approximation (or more precisely, in the adiabatic approximation) for H_2^+, with the interelectronic distance as the adiabatic parameter. The potential curves (including the rotational energy) obtained by Feagin and Briggs, each labeled by the familiar quantum numbers of those used for H_2^+, resemble the hyperspherical potential curves. Therefore there is also a one-to-one correspondence between the quantum numbers K, T, and A and those used for H_2^+.

For H_2^+, there are different sets of quantum numbers used for describing the electronic states or the potential curves. They are (a) the hydrogenic n, l, and $|m|$ quantum numbers of the united atom; (b) the N_λ, N_μ, and $\Lambda=|m|$ quantum numbers in the MO region; or (c) the Stark n_1, n_2, and $|m|$ quantum numbers in the separated-atom limit (see Ref. 54). Their relations with respect to K and T are

$$|m|=\Lambda=T\ ,$$

$$K=n_2-n_1 \tag{A2}$$

$$=\begin{cases}(n_\mu/2)-n_\lambda, & n_\mu \text{ even}\\ [(n_\mu-1)/2]-n_\lambda, & n_\mu \text{ odd}\end{cases}$$

where l and $|m|$ are related to n_λ and n_μ by $n_\lambda=n-l-1$, $n_\mu=l-|m|$.

In the ${}_n(K,T)^A_N$ designation of the doubly excited states of atoms, we also emphasize the relation between intrashell and intershell states which have identical K, T, A, and N (besides the usual L, S, and π). The quantum number A, which is *not* independent of K and T, is given by

$$A=\begin{cases}\pi(-1)^{S+T}, & K\geq L-N \quad \text{(A3a)}\\ 0, & K<L-N\ . \quad \text{(A3b)}\end{cases}$$

The $A=\pm1$ classification emphasizes the even or odd character of the (r_1-r_2) stretching mode (r_i is the distance of electron i from the nucleus), i.e., it stresses the even or odd stretch of the molecular mode of the doubly excited states of atoms. On the other hand, *not* all doubly excited states display molecular modes. There are states, designated by $A=0$, which belong to local modes and their energy levels do not display rovibrational regularity. *Only* states labeled by $A=\pm1$ exhibit rovibrational structure, or supermultiplet structure if the states are ordered in the fashion of Herrick and co-workers.[7,8] This designation also extends the supermultiplet structure to intershell states if the states belong to $A=\pm1$.

Among the three different classification schemes discussed above, only the $(K,T)^A$ scheme allows for the truncation of the rotational series explicitly. This is because K and T were obtained from a unitary transformation of the shell-model wave functions and the "remnant" of the shell model is reflected by the constraint[30]

$$K=(N-T-1),(N-T-3),\ldots,-(N-T-1)\ . \tag{A4}$$

Equation (A4), combined with (A3), determine the L's of the truncated rotor series $L=T,\ T+1,\ldots,(K+N-1)$ for each K, T, and N.

The introduction of $A=0$ in Eq. (A3) is to distinguish the class of doubly excited states which do not display any molecular modes. In fact, for states which have been designated with $A=0$, a molecular interpretation of these states is erroneous. It has been shown by Watanabe and Lin[32] that K and T are *not* approximate good quantum numbers but only served as labels for the $A=0$ states.

There is another important difference in the hyperspherical approach and the diatomic molecular approach of Feagin and Briggs. In the latter, the projection of L along the interelectronic axis was treated as an *exact* quantum number such that potential curves which have different T have *real* crossing. Since T is a good quantum number, according to (A3a), each potential curve of Feagin and Briggs is labeled with $A=\pm1$; there are no $A=0$ curves. In the hyperspherical approach T is not treated as a good quantum number and the calculated potential curves do not cross. If the dynamic consideration is included,[26,27] then the + and − hyperspherical potential curves are allowed to cross. One can say that the $A=0$ states can be obtained from the works of Feagin and Briggs if the Coriolis coupling and radial coupling are included in the calculation, i.e., by further diagonalizing their MO curves. The $A=0$ states would correspond to cases where the mixing of different T curves is large. In the language of linear triatomic molecules, the $A=0$ states correspond to the local modes, which can be obtained from the superposition of symmetric and antisymmetric molecular modes. In the hyperspherical approach, both the molecular and local modes are obtained directly from the calculation.

If one assumes that T (or Λ, or $|m|$) is a good quantum number, then the relation between the three sets of quantum numbers are given in the table below (see Ref. 24 also). The allowed values of L, S, and π along each row are given; they correspond to the rotor series in the large-λ limit. In the "atomic" ($\lambda\to0$) limit, the rotor series is truncated. Members of such a truncated series are indicated by underlines in the table. For $T\neq0$, the T-doubling states are grouped in the parentheses. The "string" of each truncted rotor series is much longer for doubly excited states converging to the higher hydrogenic excited states; see examples in Refs. 1, 7, and 8.

$(nl\|m\|)_t$	$N_\lambda N_\mu \Lambda$	$n_1 n_2 \|m\|$	vl_v	$(K,T)^A_N$	L,S,π
$2s\sigma_g$	1 0 0	1 0 0	20	$(-1,0)^+_2$	${}^1S^e,{}^3P^o,{}^1D^e,{}^3F^o,{}^1G^e,\ldots$
$3p\sigma_u$	1 1 0	1 0 0	20	$(-1,0)^-_2$	$\underline{{}^3S^e,{}^1P^o,{}^3D^e},{}^1F^o,{}^3G^e,\ldots$
$3d\sigma_g$	0 2 0	0 1 0	00	$(1,0)^-_2$	$\underline{{}^1S^e},{}^3P^o,{}^1D^e,{}^3F^o,\ldots$
$4f\sigma_u$	0 3 0	0 1 0	00	$(1,0)^-_2$	$\underline{{}^3S^e},{}^1P^o,{}^3D^e,{}^1F^o,\ldots$
$3d\pi_g$	0 1 1	0 0 1	11	$(0,1)^-_2$	$\underline{({}^1P^e,{}^3P^o)},({}^3D^o,{}^1D^e),\ldots$
$2p\pi_u$	0 0 1	0 0 1	11	$(0,1)^+_2$	$\underline{({}^3P^e,{}^1P^o)},({}^1D^o,{}^3D^e),\ldots$

TABLE I. Scaling of the ground-state binding energy (E_s) of three-body systems (AAB) with respect to the reduced mass μ of particles A and B. The column under "norm" is the ratio of E_s/μ of each system normalized to that for H^-. For the purpose of comparison, the mass of the proton in H_∞^- is assumed to be infinite. Data from Frolov, Ref. 45.

System	E_s (a.u.)	μ	λ	norm
H_∞^-	0.527 75	1.0	5.446×10^{-4}	1.000
$e\mu e$	0.525 054	0.9952	0.0048	0.9997
$\pi\pi K$	111.3879	212.932	0.2827	0.9912
$e(3e)e$	0.392 14	0.75	0.3333	0.9907
$e(2e)e$	0.348 37	0.6667	0.5	0.9902
pKK	330.8119	633.051	0.5262	0.9902
eee	0.262 005	0.5	1.0	0.9929
ppK	334.5864	633.051	1.9004	1.0015
πKK	114.107 43	212.932	3.5373	1.0154
$pp\pi$	129.715 88	237.760	6.7227	1.0338
$pp\mu$	102.229 85	185.78	8.8887	1.0427
$dd\mu$	109.8237	195.68	17.762	1.0635
$tt\mu$	112.9799	199.21	26.596	1.0746
H_2^+	0.592 01	1.0	1836.2	1.1218

APPENDIX B: REDUCED-MASS SCALING OF GROUND-STATE ENERGIES OF COULOMBIC THREE-BODY SYSTEMS

The Hamiltonian for the Coulombic three-body system AAB can be expressed in terms of the two vectors $\mathbf{r}_1$ and $\mathbf{r}_2$ from B to each of the particles A,

$$H=\frac{m}{1+m/M}\left[-\frac{1}{2}\nabla_1^2-\frac{1}{2}\nabla_2^2-\frac{1}{r_1}-\frac{1}{r_2}+\frac{1}{r_{12}}\right] -\frac{m^2/M}{(1+m/M)^2}\nabla_1\cdot\nabla_2$$
$$=\mu[H_\infty+(\mu/M)\mathbf{p}_1\cdot\mathbf{p}_2]\ , \tag{B1}$$

where $M=m_B$ and H_∞ is the Hamiltonian when the mass of particle B is assumed to be infinite. The second term in the expression above is the mass-polarization interaction resulting from the correction of the motion of the two A particles with respect to the center of mass of the AAB system. If the mass-polarization term is small, then the binding energy calculated from (B1) is proportional to the reduced mass μ.

Mass polarization is small when the expectation value of $(\mu/M)\langle\mathbf{p}_1\cdot\mathbf{p}_2\rangle$ is small compared with the ground-state energy. For $\lambda=(m/M)\ll1$, μ/M is small and the scaling with respect to μ is expected. Physically this is understood since the center of mass is very close to particle B and thus the correction is small. This is not so obvious for Ps^- where the three particles have identical masses. The validity of μ scaling must therefore rely on the smallness of $\langle\mathbf{p}_1\cdot\mathbf{p}_2\rangle$. For all the three-body systems where $\lambda\le1$ the momentum correlation is expected to be small and thus the ground-state energy nearly scales with μ. As λ increases, we note that the center of mass begins to deviate further from B. In the molecular limit such as in H_2^+, the mass-polarization term is very large. This can be understood from the nature of the bonding orbital. Since the electron is required to have larger charge density between the two protons, this implies that $\mathbf{r}_1$ and $\mathbf{r}_2$ are to remain on opposite directions most of the time, thus the expectation value $(\mu/M)\langle\mathbf{p}_1\cdot\mathbf{p}_2\rangle$ is negative, which results in tighter binding.

In Table I we check the validity of the μ scaling for the various Coulombic three-body systems. The ground-state energies listed are adopted from the results of Frolov (Ref. 45) who used Hylleraas-type basis functions in a variational calculation. If the μ scaling is exact, the last column should be equal to 1. We note that deviations from 1 is very small for $\lambda\le1$, no greater than 1% in all the entries shown. As λ becomes greater than unity, the μ scaling is no longer accurate. The ratio is greater than 1 meaning that the system is more tightly bound in comparison to H^-, which is in agreement with the interpretation of the mass-polarization term in the preceding paragraph.

[1]C. D. Lin, Adv. Mol. Phys. **22**, 77 (1986).
[2]U. Fano, Rep. Prog. Phys. **46**, 97 (1983).
[3]J. W. Cooper, U. Fano, and F. Prats, Phys. Rev Lett. **10**, 518 (1963).
[4]D. R. Herrick, Adv. Chem. Phys. **52**, 1 (1983).
[5]R. S. Berry, Contemp. Phys. **30**, 1 (1989).
[6]M. E. Kellman and D. R. Herrick, J. Phys. B **11**, L755 (1978).
[7]M. E. Kellman and D. R. Herrick, Phys. Rev. A **22**, 1536 (1980).
[8]D. R. Herrick, M. E. Kellman, and R. D. Poliak, Phys. Rev. A **22**, 1517 (1980).
[9]J. H. Macek, J. Phys. B **1**, 831 (1968).
[10]R. S. Berry and J. L. Krause, Adv. Chem. Phys. **70**, 35 (1988).
[11]H. J. Yuh, G. S. Ezra, P. Rehmus, and R. S. Berry, Phys. Rev. Lett. **47**, 497 (1981).
[12]G. S. Ezra and R. S. Berry, Phys. Rev. A **28**, 1974 (1983).
[13]J. L. Krause, J. D. Morgan III, and R. S. Berry, Phys. Rev. A **35**, 3189 (1987).

[14]J. E. Hunter III and R. S. Berry, Phys. Rev. A **36**, 3042 (1987).
[15]J. E. Hunter III and R. S. Berry, Phys. Rev. Lett. **59**, 2959 (1987).
[16]M. E. Kellman, Phys. Rev. Lett. **31**, 1783 (1985).
[17]C. D. Lin, in *Fundamental Processes of Atomic Dynamics,* edited by J. S. Briggs, H. Kleinpoppen, and H. O. Lutz (Plenum, New York, 1988).
[18]J. Feagin and J. S. Briggs, Phys. Rev. Lett. **57**, 984 (1987).
[19]J. Feagin, Ref. 17, p. 275.
[20]K. Molmer and K. Taulbjerg, J. Phys. B **21**, 1739 (1988).
[21]D. R. Herschbach, J. G. Loeser, and D. K. Watson, Z. Phys. D **10**, 195 (1988).
[22]C. D. Lin, Phys. Rev. A **29**, 1019 (1984).
[23]C. D. Lin, Phys. Rev. Lett. **51**, 1348 (1983).
[24]J. Feagin and J. S. Briggs, Phys. Rev. A **37**, 4599 (1988).
[25]J. M. Rost and J. S. Briggs, Z. Phys. D **5**, 339 (1988).
[26]N. Koyama, H. Fukuda, T. Motoyama, and M. Matsuzawa, J. Phys. B **19**, L331 (1986).
[27]H. Fukuda, N. Koyama, and M. Matsuzawa, J. Phys. B **20**, 2959 (1987).
[28]C. H. Greene, Phys. Rev. A **23**, 661 (1981).
[29]S. Watanabe, Phys. Rev. A **25**, 2074 (1982).
[30]D. R. Herrick and O. Sinanoğlu, Phys. Rev. A **11**, 97 (1975).
[31]C. Wulfman, Chem. Phys. Lett. **23**, 370 (1973).
[32]S. Watanabe and C. D. Lin, Phys. Rev. A **34**, 823 (1986).
[33]Z. Chen and C. D. Lin, J. Phys. B **22**, 2875 (1989).
[34]C. D. Lin, J. Phys. B **16**, 723 (1983).
[35]Z. Chen and C. D. Lin, Phys. Rev. A **40**, 6712 (1989).
[36]M. Dunn, Z. Chen and C. D. Lin (unpublished).
[37]A. P. Mills, Phys. Rev. Lett. **46**, 717 (1981).
[38]Y. K. Ho, Phys. Lett. **A102**, 348 (1984).
[39]A. K. Bhatia and R. J. Drachman, Phys. Rev. A **28**, 2523 (1983).
[40]See, for example, *Muon-catalyzed Fusion, Proceedings of a Conference on Muon-Catalyzed Fusion, Sanibel Island, Florida, 1988,* AIP Conf. Proc. No. 181, edited by Steven E. Jones, Johann Rafelski, and Hendrik J. Monkhorst (AIP, New York, 1989).
[41]C. D. Lin and X. H. Liu, Phys. Rev. A **37**, 2749 (1987).
[42]C.-G. Bao, Y.-P. Gan, and X.-H. Liu, Comput. Phys. Commun. **36**, 410 (1985).
[43]R. T. Pack and G. A. Parker, J. Chem. Phys. **87**, 3888 (1987); **90**, 3511 (1989); see also B. J. Archer, G. A. Parker, and R. T. Pack, Phys. Rev. A **41**, 1303 (1990).
[44]J. Botero and C. H. Greene, Phys. Rev. Lett. **56**, 1366 (1986).
[45]The most extensive calculation was done by A. M. Frolov, Zh. Eksp. Teor. Fiz. **92**, 1959 (1987) [Sov. Phys.—JETP **65**, 1100 (1987)].
[46]G. Hunter, A. W. Yau, and H. O. Pritchard, At. Nucl. Data Tables **14**, 11 (1974), and references therein.
[47]A. K. Bhatia and D. J. Drachman, Phys. Rev. A **35**, 4051 (1987).
[48]See H. S. W. Massey and E. H. S. Burhop, *Electronic and Ionic Impact Phenomena* (Oxford University Press, New York, 1969), Vol. I, p. 518, Fig. 8.1.
[49]S. J. Ward, J. W. Humberston, and M. R. C. McDowell, J. Phys. B **20**, 127 (1987).
[50]S. Watanabe and C. D. Lin, Phys. Rev. A **36**, 511 (1987).
[51]Y. Komninos, M. Chrysos, and C. A. Nicolaides, Phys. Rev. A **38**, 3182 (1988).
[52]J. Botero and C. H. Greene, Phys. Rev. A **32**, 1249 (1985); J. Botero, *ibid.* **35**, 36 (1987).
[53]J. Botero, Z. Phys. D **8**, 177 (1988).
[54]D. R. Bates and R. H. G. Reid, Adv. At. Mol. Phys. **4**, 13 (1968).
[55]C. D. Lin, Phys. Rev. Lett. **35**, 1150 (1976).
[56]G. S. Ezra and R. S. Berry, Phys. Rev. A **28**, 197 (1983).